Cell Reports, Volume *39*

Supplemental information

Global post-translational modification profiling of HIV-1-infected cells reveals mechanisms of host cellular pathway remodeling

Jeffrey R. Johnson, David C. Crosby, Judd F. Hultquist, Andrew P. Kurland, Prithy Adhikary, Donna Li, John Marlett, Justine Swann, Ruth Hüttenhain, Erik Verschueren, Tasha L. Johnson, Billy W. Newton, Michael Shales, Viviana A. Simon, Pedro Beltrao, Alan D. Frankel, Alexander Marson, Jeffery S. Cox, Oliver I. Fregoso, John A.T. Young, and Nevan J. Krogan

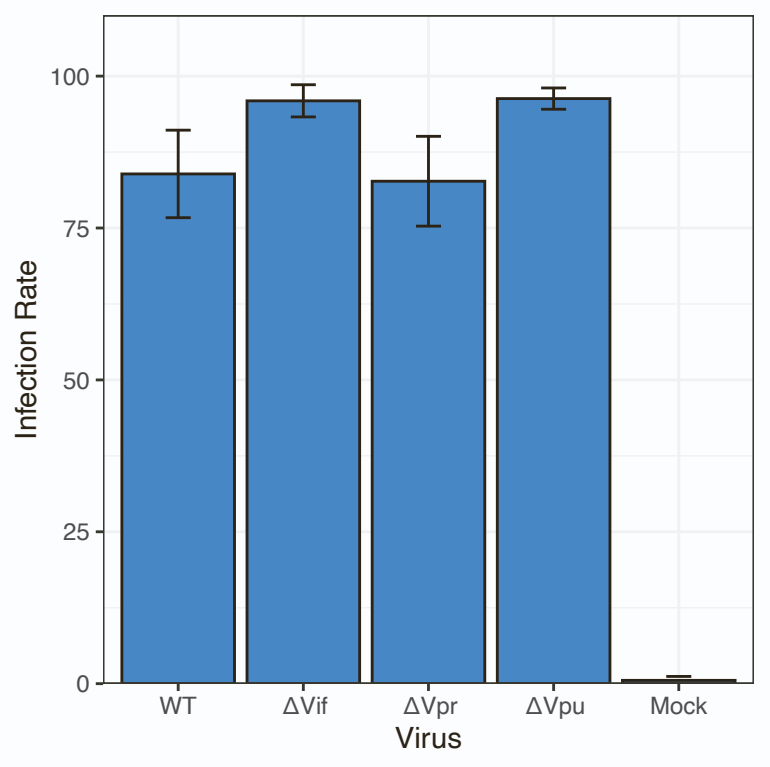

Figure S1. Infection rates of viruses used in this study. Jurkat E6.1 cells were infected with VSVG=pseudotyped, ΔEnv HIV-1 (strain NL4-3) with the indicated mutations at an MOI of 5 (n = 3 biological replicates). Mock virus was ΔEnv HIV-1 without pseudotyping. Cells were fixed and intracellularly stained with anti-p24 FITC-conjugated antibody and infection rates assessed by flow cytometry. Related to Figure 1.

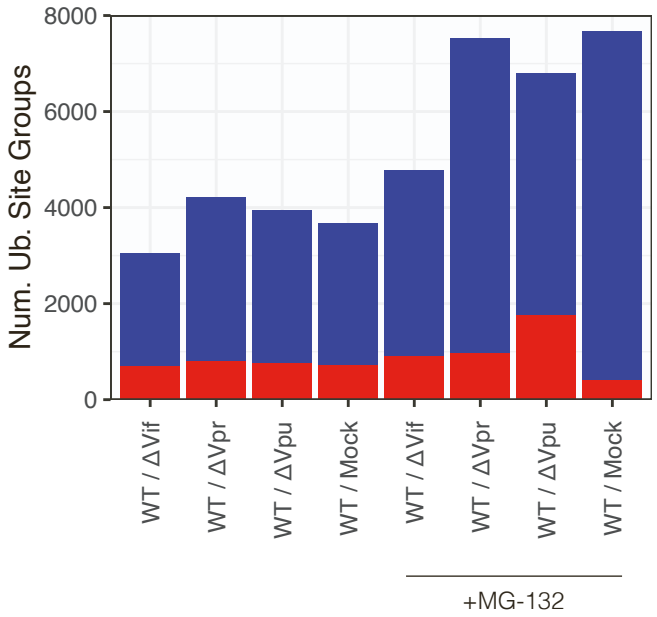

Figure S2. Quantification of ubiquitination SILAC ratios in forward and reverse orientations. The number of ubiquitination sites that were quantified in SILAC experimenta in only one direction (red) and in both directions (blue) in each of the indicated experimental conditions. Related to Figure 1.

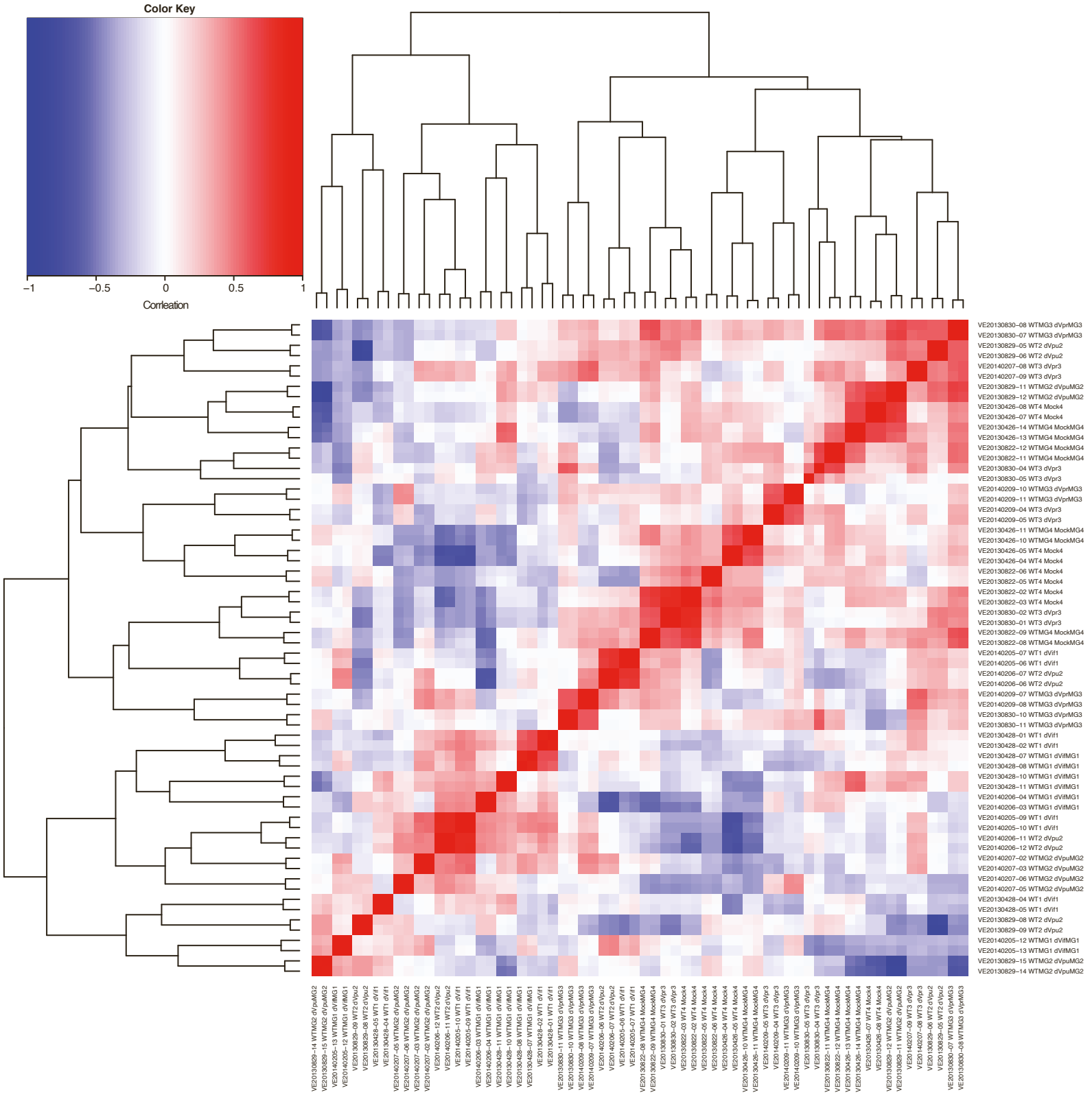

Figure S3. Correlation analysis of ubiquitination $\log_2$fold-change profiles. Pearson correlation coefficients are indicated by the color scale for every samples vs. every sample. Data were ordered by hierarchical clustering based on Euclidian distances. Related to Figure 1.

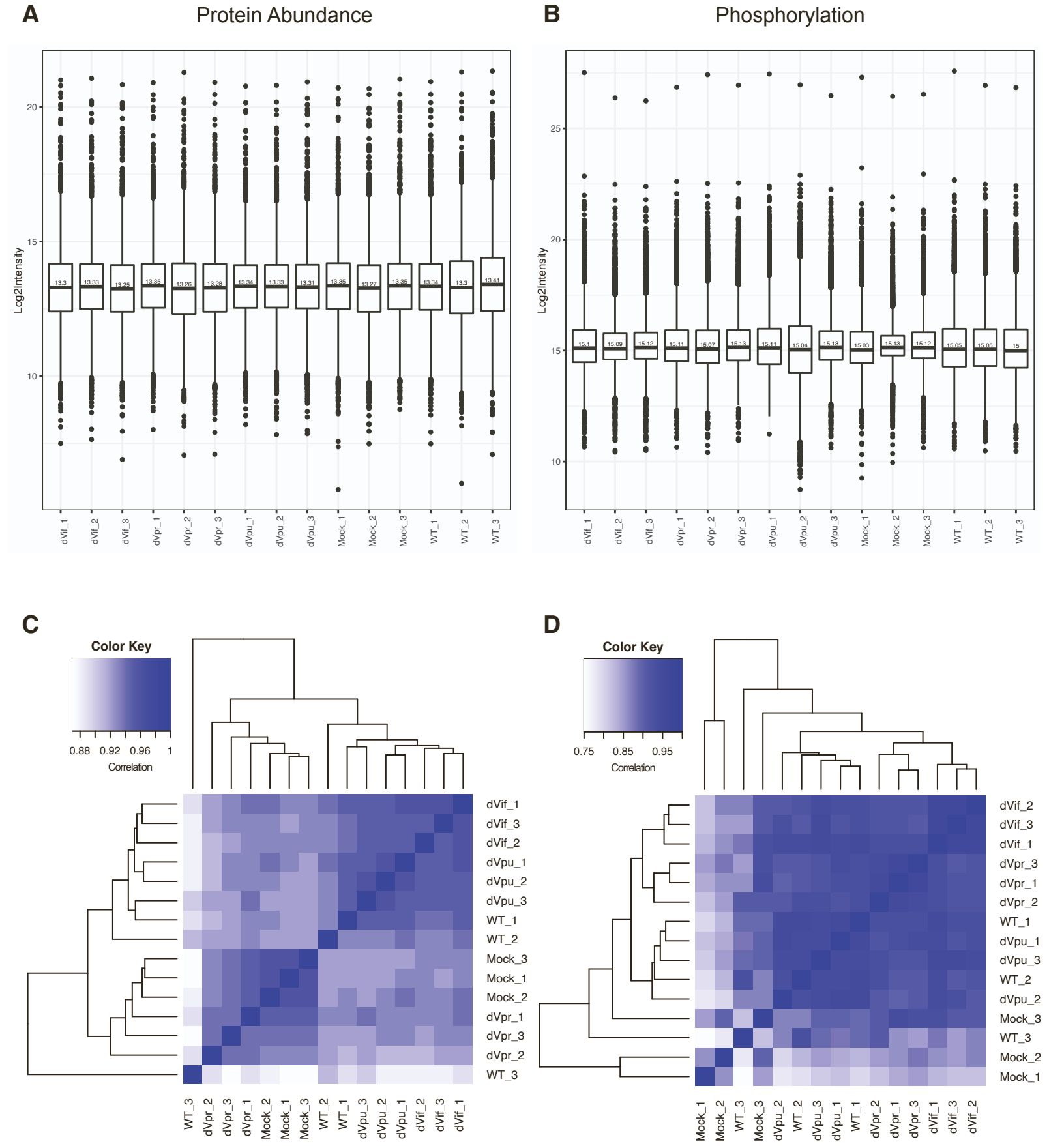

Figure S4. Quality control plots for global protein abundance and phosphoproteomics data. (A-B) Box plots of $\log_2$intensities for protein abundance (A) and phosphoproteomics (B) samples from cells infected with WT, ΔVif, ΔVpr, ΔVpu, or mock virus (n = 3 biological replicates). The median $\log_2$intensity is indicated in each box. (C-D) Sample correlation analysis of $\log_2$intensity profiles for protein abundance (C) and phosphoproteomics (D) samples from cells infected with WT, ΔVif, ΔVpr, ΔVpu, and mock virus. Related to Figure 1.

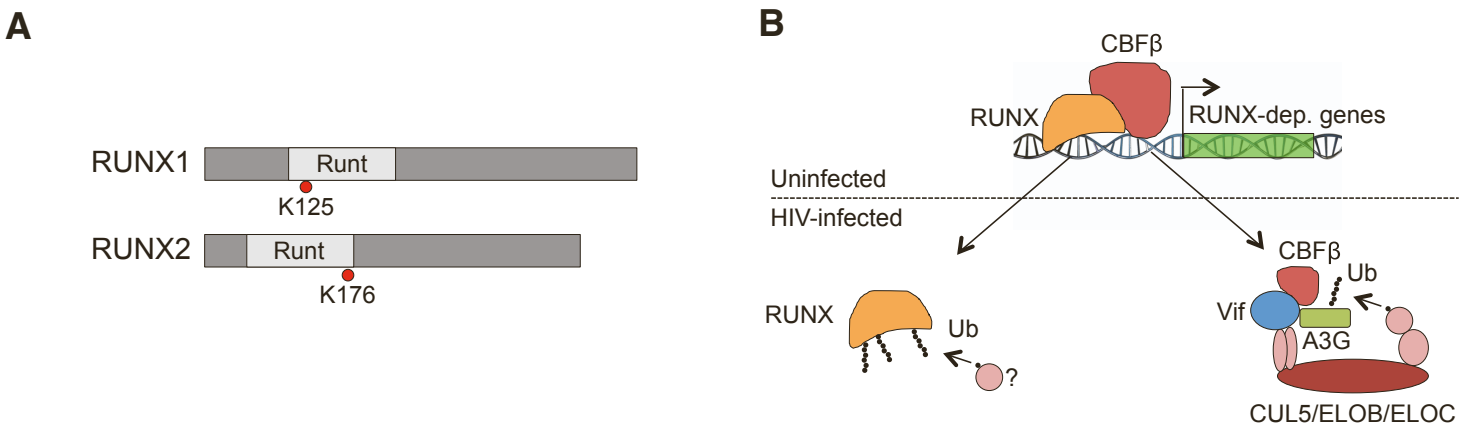

Figure S5. Ubiquitination of RUNX transcription factors. (A) Schematic of ubiquitination sites detected on RUNX1 and RUNX2. The Runt domain of each is indicated in light gray. (B) Proposed model for ubiquitination of RUNX proteins. HIV-1 Vif sequesters the RUNX binding partner CBFβ, which destabilizes RUNX and leads to ubiquitination. Related to Figure 2.

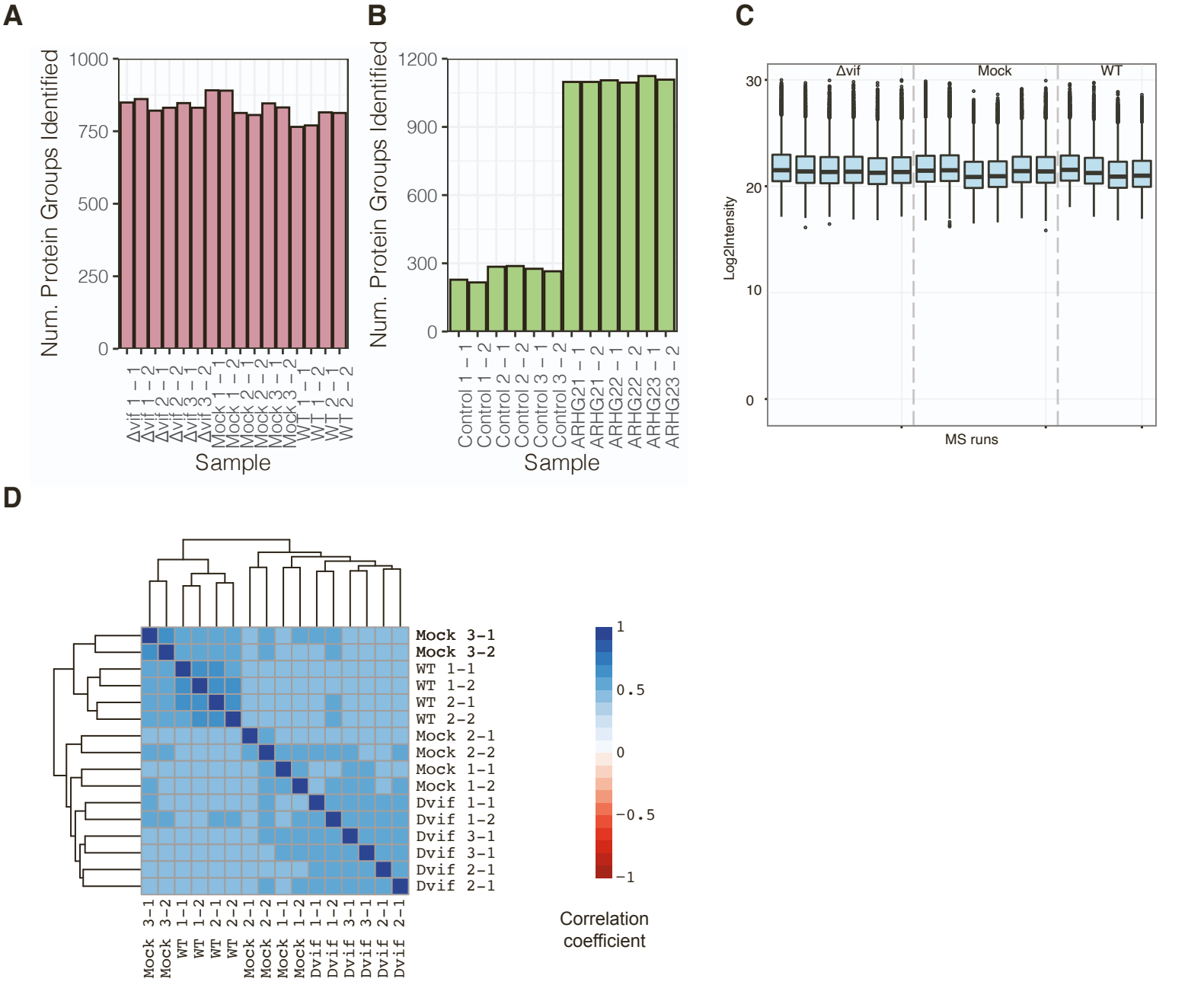

Figure S6. Quality control plots for samples associated with ARHG2 interaction analysis. (A) Protein groups identifications for ARHG2 IP-MS samples from Jurkat E6.1 cells infected with WT, ΔVif, and mock virus (n = 3 biological replicates). (B) Protein group identifications for IP-MS samples from uninfected cells with isotype control or ARHG2 antibody (n = 3 biologicl replicates). (C) Box plots of $\log_2$intensities for ARHG2 IP-MS samples comparing WT, ΔVif, and mock infection. (D) Sample correlation analysis of $\log_2$intensity profiles for ARHG2 IP-MS samples comparing WT, ΔVif, and mock infection. Related to Figure 5.

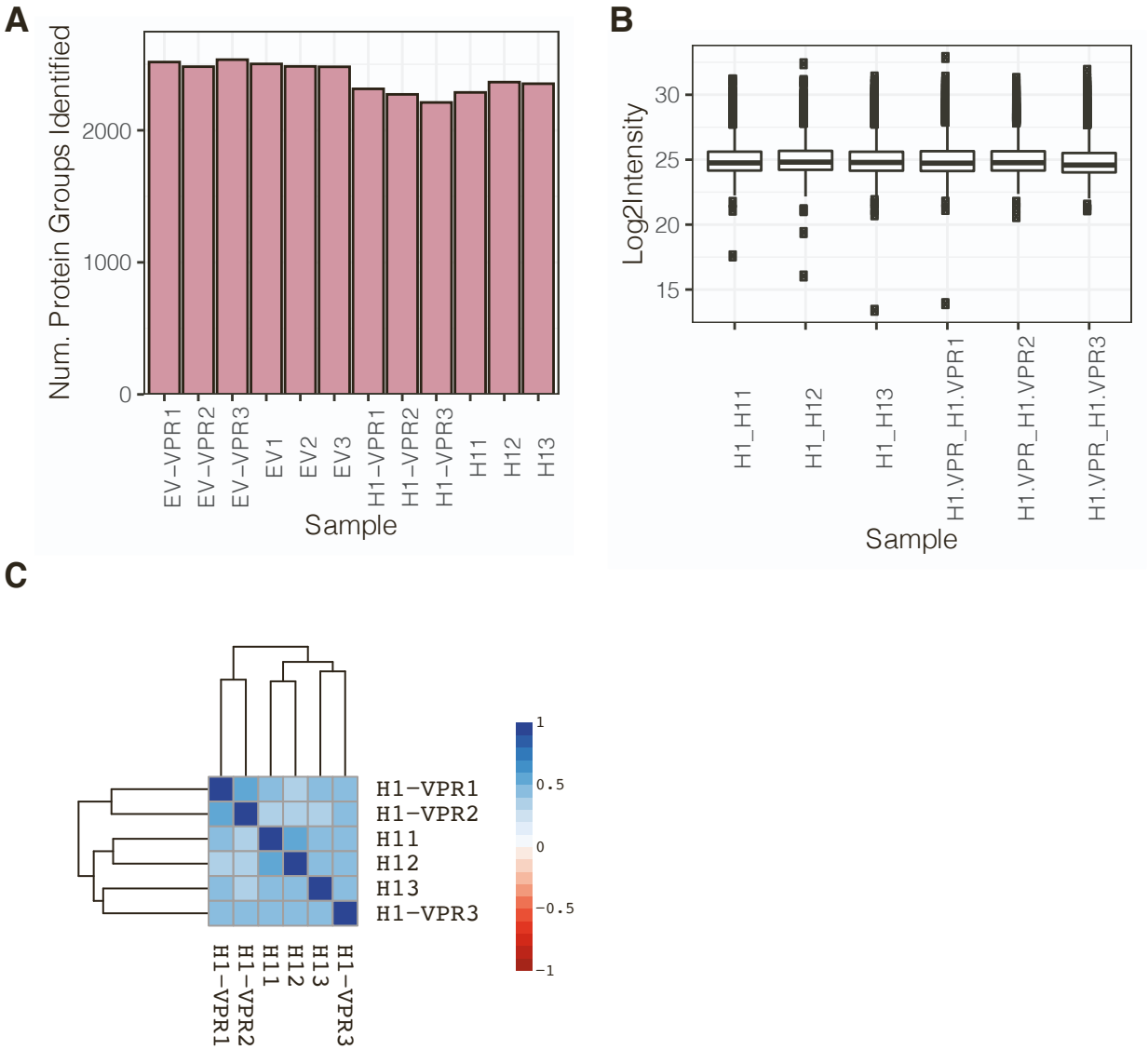

Figure S7. Quality control plots for samples associated with histone H1.2 interaction analysis. (A) Protein group identifications for histone H1.2 AP-MS from HEK293T cells co-transfected with histone H1.2 (H1) and empty vector (EV) or Vpr (n = 3 biological replicates). (B) Box plots of $\log_2$intensities for histone H1.2 AP-MS samples from cells co-transfected with histone H1.2 (H1) and empty vector or Vpr. (C) Sample correlated analysis of $\log_2$intensity profiles for histone H1.2 AP-MS samples from cell co-transfected with histone H1.2 (H1) and empty vector or Vpr. Related to Figure 6.